

Single-shot phase-shifting on Michelson interferometry for incoherent digital holography

Keehoon Hong  | Kihong Choi

Digital Holography Research Section,
Electronics and Telecommunications
Research Institute, Daejeon, Republic of
Korea

Correspondence

Keehoon Hong, Digital Holography
Research Section, Electronics and
Telecommunications Research Institute,
Daejeon, Republic of Korea.
Email: khong@etri.re.kr

Funding information

This research was supported by the
Institute for Information and
Communications Technology Promotion
(2019-0-00001).

Abstract

A single-shot phase-shifting method in incoherent digital holography (IDH) based on Michelson interferometry is proposed herein. The proposed method uses polarization-modulating optical elements and a polarization sensor in the Michelson interferometer optics to induce a geometric phase shift. It acquires four holograms with different geometric phase retardations in a single exposure to eliminate the bias and conjugate noise using a phase-shifting technique. The proposed optical system enables real-time bias and conjugate term removal from a recorded hologram without requiring sequential recording for phase shifting. Furthermore, because it is based on Michelson interferometry, it can be implemented using simple reflective optics without expensive or difficult-to-produce optical elements for single-shot phase shifting. The principles of self-interference and geometric phase shifting in the proposed optical structure were analyzed mathematically. A real-time IDH-recording experimental setup was constructed to verify the proposed method. The experimental results of single-shot phase-shifting IDH and hologram movie recordings confirm the feasibility of the proposed method.

KEYWORDS

geometric phase, incoherent digital holography, Michelson interferometry, self-interference, single-shot phase-shifting

1 | INTRODUCTION

Incoherent digital holography (IDH) is a promising three-dimensional imaging technique that allows the capturing of hologram information using the principle of self-interference under low-coherence light conditions without the need for a laser light source [1, 2]. Research on IDH has gained attention in microscopic applications because it can overcome the limitations of conventional optical physics by exploiting the violations of the Lagrange invariant [3]. Research on IDH for holographic

camera applications has been actively conducted since Kim proposed the natural light holographic camera concept [4] which exploits the advantages of IDH in capturing holograms under a variety of outdoor light conditions.

Major applications of IDH, such as in microscopy and holographic cameras, aim to acquire the hologram information of moving objects or dynamic scenes without any severe noise, such as bias and conjugate image noise, which are inherent in holographic interferometry. Off-axis configured interferometry is a possible solution to

the problems of bias and conjugate noise in IDH [5, 6]. In a previous off-axis IDH study, they tilted one of the mirrors on the interferometer from the on-axis position to extract the bias and conjugate spectral components and recorded only the object information on the hologram, as in conventional off-axis holography. However, it is difficult to use these methods for the construction of simple inline optical structures. Furthermore, it has a reduced area of recordable holograms because the off-axis configuration increases the optical path length difference between the two beam paths in interferometry under the short temporal coherence-length condition of natural light illumination. Iterative phase retrieval methods are another approach used to reduce this noise in holographic imaging [7]. Although this method applies phase-retrieval algorithms to incoherent holography with compact imaging optics, it requires additional computation time for iterations, which prohibits real-time imaging. In addition, most iterative phase-retrieval methods have a lens-less configuration, which is suitable for microscopy but difficult to apply in holographic camera applications.

Conversely, the phase-shifting technique can accurately eliminate the bias and conjugate image noise without these issues; therefore, it is extensively used in coherent digital holography [8]. Among various phase-shifting techniques, sequential phase shifting was first applied to IDH. These previous studies recorded multiple holograms with different phase retardations for the phase-shifting method in a stepwise manner by adjusting the path length difference using a mirror mounted on a piezotransducer [4], changing the phase modulation patterns with different phase-shift values [9], and rotating the polarizer or waveplate to induce a geometric phase delay [10]. Therefore, IDH with sequential phase shifting can only record static information and is impractical for dynamic incoherent hologram imaging. To overcome the difficulty of real-time acquisition in sequential phase-shifting IDH, various single-shot phase-shifting holography techniques have been reported [11–16]. In these previous single-shot phase-shifting IDH studies, diffractive phase gratings [13, 14], coded aperture [12, 16], birefringence [15], geometric phase [11] optical elements, and liquid-crystal-based optical devices [17] have been employed in the optical system to achieve real-time phase-shifting instead of the simple reflective optical components used in interferometry-based IDH methods [4, 18, 19].

Recent research focused on the implementation of quasi-real-time phase shifting by accelerating holographic acquisition during sequential phase-shifting procedures [20] and the increase of the optical efficiency of IDH by polarization-multiplexed phase shifting without

using any polarization filters [21]. However, to achieve such advancements in these studies, additional optical components, such as fast-switching phase modulation devices and high frame-rate sensors for quasi-real-time acquisition, and at least two liquid crystal on silicon (LCoS) are required for polarization multiplexing.

Single-shot phase shifting in IDH is feasible using the approaches described above; however, several notable drawbacks must be considered. First, one of the main drawbacks is the high cost and difficulty of manufacturing optical elements associated with the implementation of these techniques compared with classical optics, such as lenses and mirrors used in conventional interferometry. Another challenge arises from the color dispersion that can occur within optical elements, such as diffractive phase gratings, birefringence optics, and liquid-crystal-based geometric phase lenses used in these IDH systems. This dispersion can lead to undesirable effects, such as chromatic aberration and depth distortion in the reconstructed images, as the wavelength of the illuminating light varies. In addition, spatial multiplexing with diffractive phase gratings for single-shot phase-shifting IDH introduces additional complexity in terms of the alignment in the optical system. Although several studies have reported simultaneous phase shifting using optical configurations combining a Michelson interferometer and polarization-modulating optical elements [22–24], to our knowledge, there have been no attempts to use them to acquire three-dimensional information in real-time from objects located outside the interferometer's optical paths under incoherent light conditions.

In this study, we propose a single-shot phase-shifting method for IDH based on a Michelson interferometry structure. A geometric phase shift was achieved by combining the polarization-modulating optical elements in the proposed optical system. As the proposed method is based on the optical structure of the Michelson interferometer, which consists of reflective optical elements, it is cost-effective and easy to implement. Furthermore, our optical system enables single-shot phase-shifting holography within the IDH framework. The incorporation of polarization-modulating optical elements and a polarization sensor enables the simultaneous acquisition of four different phase-shifted holograms, thus making real-time hologram acquisition possible. First, we introduce the principles of self-interference and geometric phase-shifting in the proposed optical structure. Thereafter, we describe an optical system for real-time capture of holograms that implements the proposed principle. Finally, the feasibility of the proposed single-shot phase-shifting holography applied in IDH was experimentally verified by capturing hologram movies of a dynamic scene using the proposed optical system.

2 | METHODS

2.1 | Optical structure of proposed single-shot phase-shifting IDH system

The overall configuration of the proposed optical system was based on a Michelson interferometer. The optical system for the proposed method has two notable differences from the previous Michelson interferometry-based IDH [4, 18] in terms of achieving geometric phase retardation in the beam paths. Geometric phase retardation does not introduce any changes in the beam path compared with dynamic phase retardation. Therefore, it is suitable for applying phase shifting to IDH, which has inherent limitations in the optical path-length difference owing to the short temporal coherence length of low-coherence light conditions. It can also improve the system's stability by replacing the conventional mechanical movement required for dynamic phase shifting, which involves the adjustment of the optical path using polarization-modulating optics. The first is the presence of polarization-modulating optical elements in the optical configuration. In the proposed optical system, linear polarizers, polarization beam splitter, and quarter-wave plates (QWPs) located at the transmitted, reflected, and recombined beam paths were employed in conventional Michelson interferometry. The second is the use of a polarization sensor for the detector instead of a conventional sensor, such as a charge-coupled device or complementary metal-oxide semiconductor. Polarization sensors use a micropolarizer array (PA), which consists of four angled polarizers placed at each pixel in the sensor plane to capture images of polarized light in four directions in a single acquisition. Typically, the PA in a polarization sensor is configured to have linear polarization states of 0° , 45° , 90° , and 135° to allow calculation of the angle and degree of linear polarization required for polarization image analysis. The proposed method utilizes a combination of polarization-modulating optics and polarization sensors to generate geometric phase retardation and simultaneously capture four phase-shifted holograms. Detailed explanations of the principles of single-shot phase-shifting are provided in Section 2.3.

A schematic of the optical arrangement in the proposed method is shown in Figure 1. The objects in the scene are illuminated by spatially and temporally incoherent light, and the scattered light from the object is collected by a field lens with focal length f_0 and then incident onto the interferometer optics. To enhance the temporal coherence of the incoming light, which is required for self-interference in the IDH, a bandpass filter with a central wavelength λ was employed in the optical system to enhance the temporal coherence of the

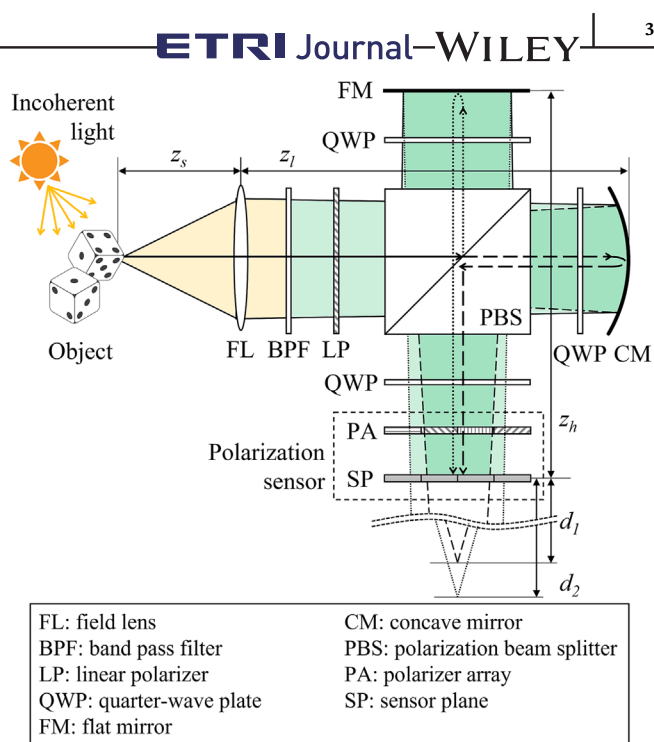


FIGURE 1 Schematic of the proposed single-shot phase-shifting incoherent digital holography (IDH) with Michelson interferometry.

incoming light, which is required for self-interference in IDH. Subsequently, a linear polarizer was used to define the initial polarization state and control the split ratio of transmitted and reflected light using a polarization beam splitter (PBS). In this configuration, the transmission axis of the linear polarizer was aligned at 45° to set the split ratio to 50:50. A flat mirror (FM) and concave mirror (CM) with a focal length of f_c were placed at the end of each beam path on the interferometer. Two QWPs were located between the PBS and the CM/FM mirrors on each beam path of the interferometer to convert, respectively, the horizontal and vertical linearly polarized light from the PBS into left and right circularly polarized light. The polarization states on each beam path were changed to orthogonal circular polarization by mirror reflection and converted back into linear polarization in the vertical and horizontal directions by the previous QWPs. Subsequently, the linearly polarized light on each beam path was recombined by the PBS and incident on another QWP located between the PBS and the polarization sensor. The light from each path with left/right circular polarization, after passing through the last QWP, was recorded in the sensor plane as four holograms with common linear polarization plane states (0° , 45° , 90° , and 135°) defined by the linear polarizer array in the polarization sensor.

The distances from the object to the field lens, the field lens to the mirrors, and the mirrors to the sensor

plane are defined as z_s, z_l , and z_h , respectively. The distances from the sensor plane to the image positions of the point light source formed by the combination of the field lens and CM/FM are denoted as d_1 and d_2 , respectively.

2.2 | Principles of incoherent self-interference in proposed method

The hologram acquired by the IDH optical system can be regarded as an accumulation of self-interfering holograms from spatially incoherent point lights comprising an object. For simplicity, the principles of self-interference and geometric phase shifting in the proposed method are described with single point light source object. A self-interfering hologram (I_n) from a point light source captured by the proposed optical system can be mathematically represented as

$$I_n = |\Psi_r|^2 + |\Psi_t|^2 + \Psi_r \Psi_t^* \exp(j\delta_n) + \Psi_r^* \Psi_t \exp(-j\delta_n), \quad (1)$$

where Ψ_r and Ψ_t are the optical fields propagated through the reflected and transmitted beam paths in the Michelson interferometer, respectively, and δ_n is the geometric phase induced by the proposed optical system, which will be discussed later. The optical fields Ψ_r and Ψ_t are expressed as follows:

$$\begin{aligned} \Psi_r(\vec{r}) &= C_1 L\left(\frac{-\vec{r}}{z_s}\right) Q\left(\frac{1}{z_s}\right) Q\left(\frac{-1}{f_o}\right) * Q\left(\frac{1}{z_l + z_h}\right), \\ \Psi_t(\vec{r}) &= C_2 L\left(\frac{-\vec{r}}{z_s}\right) Q\left(\frac{1}{z_s}\right) Q\left(\frac{-1}{f_o}\right) * Q\left(\frac{1}{z_l}\right) Q\left(\frac{-1}{f_c}\right) * Q\left(\frac{1}{z_h}\right), \end{aligned} \quad (2)$$

where $*$, \vec{r} , C , $Q(\alpha) = \exp\{j\pi\alpha(x^2 + y^2)/\lambda\}$ and $L(\vec{\alpha}) = \exp\{j2\pi(\alpha_x x + \alpha_y y)/\lambda\}$ are a convolution operator, position vector, complex coefficient, quadratic phase function, and linear phase function, respectively. By substituting (2) into (1), I_n can be rewritten as

$$I_n(\vec{r}) = C_3 + C_4(\vec{r}) Q\left(-\frac{1}{z_r}\right) L\left(\frac{M\vec{r}}{z_r}\right) \exp(j\delta_n) + \text{c.c.}, \quad (3)$$

where C_3, C_4 , and c.c. denote the bias image, complex coefficient, and conjugate term, respectively. Furthermore, z_r and M are the reconstruction distance and optical magnification factor of the recorded hologram,

respectively. The image distances of the flat and concave mirrors, d_1 and d_2 , as illustrated in (1) can be defined as follows:

$$\begin{aligned} d_1 &= \frac{(z_s + z_l)f_o - z_s z_l}{z_s - f_o}, \\ d_2 &= \frac{f_c d_1}{f_c + d_1}. \end{aligned} \quad (4)$$

The reconstruction distance of the recorded hologram z_r can be calculated using the lens in (4) as follows:

$$\frac{1}{z_r} = \frac{1}{z_h - d_1} + \frac{1}{z_h - d_2}. \quad (5)$$

In this optical system, the optical magnification M is defined as [25]

$$M = \frac{z_h f_o}{(z_s + z_l)f_o - z_s z_l}. \quad (6)$$

Because a single-point light object generates a Fresnel hologram, as described in (3), the entire hologram of the object scene can be calculated by accumulating a group of object points on the scene. However, the two terms remain separate from the desired complex hologram information, that is, the bias and conjugate components, and these unwanted components should be removed. In the following section, the principles of the single-shot phase-shifting algorithm for the proposed optical system to remove bias and conjugate terms in real time are presented.

2.3 | Single-shot phase-shifting in proposed method

The bias and conjugate terms in Equation (3) can be removed by the phase-shifting technique using multiple (n) holograms (I_n), which have different phase retardation values, δ_n . The principle of the proposed method used to acquire four holograms ($n = 4$) with different phase-shifting values in a single acquisition can be explained by the Jones matrix calculation. The Jones transfer matrices for each transmitted and reflected beam path, T_t and T_r , from the end of the linear polarizer located at the entrance of the proposed optical system to the sensor plane after the linear polarizer array in the polarization sensor can be defined as follows:

$$\begin{aligned} T_t &= T_{L(\theta)} T_{Q(45)} T_{PBS(s)} T_{Q(-45)} T_M T_{Q(45)} T_{PBS(p)}, \\ T_r &= T_{L(\theta)} T_{Q(45)} T_{PBS(p)} T_{Q(-45)} T_M T_{Q(45)} T_{PBS(s)}. \end{aligned} \quad (7)$$

Details of the Jones transfer matrices for the QWPs (T_Q), polarization beam splitter (T_{PBS}), mirror (T_M), and linear polarizer array ($T_{L(\theta)}$) are listed in Table 1.

When the linearly polarized object light by the linear polarizer with a 45° transmission axis (Jones vector of $\frac{1}{\sqrt{2}} \begin{bmatrix} 1 \\ 1 \end{bmatrix}$) is incident into the proposed optical system, the optical fields Ψ_t and Ψ_r on the image sensor plane can be described by the following equations:

$$\begin{aligned} \Psi_t &= \frac{e^{j\pi/2}}{2\sqrt{2}} \begin{bmatrix} \cos^2\theta_n & \cos\theta_n \sin\theta_n \\ \cos\theta_n \sin\theta_n & \sin^2\theta_n \end{bmatrix} \begin{bmatrix} 1 \\ j \end{bmatrix}, \\ \Psi_r &= \frac{1}{2\sqrt{2}} \begin{bmatrix} \cos^2\theta_n & \cos\theta_n \sin\theta_n \\ \cos\theta_n \sin\theta_n & \sin^2\theta_n \end{bmatrix} \begin{bmatrix} 1 \\ -j \end{bmatrix}. \end{aligned} \quad (8)$$

The above equation indicates that the polarization states, after they pass through the transmitted and reflected beam paths, are changed to right- and left-handed circular polarizations (Jones vectors of $\frac{1}{\sqrt{2}} \begin{bmatrix} 1 \\ j \end{bmatrix}$ and $\frac{1}{\sqrt{2}} \begin{bmatrix} 1 \\ -j \end{bmatrix}$), respectively, and then incident to the linear polarizer array in the polarization sensor. The orthogonally circularly polarized light of each beam path was converted to common linear polarization states using linear polarizers with four different transmission angles θ_n . After the linear polarizer array in the polarization sensor, the Jones vectors for the optical fields Ψ_t and Ψ_r in the image sensor plane are defined as follows:

$$\begin{aligned} \Psi_t &\propto e^{j\theta_n} \begin{bmatrix} \cos\theta_n \\ \sin\theta_n \end{bmatrix}, \\ \Psi_r &\propto e^{-j\theta_n} \begin{bmatrix} \cos\theta_n \\ \sin\theta_n \end{bmatrix}. \end{aligned} \quad (9)$$

Accordingly, the intensity of the hologram recorded with these two optical fields can be rewritten as

$$I_n(\theta_n) = |\Psi_t + \Psi_r|^2 \propto 1 + \cos(2\theta_n). \quad (10)$$

Therefore, the phase shift value of δ_n in (1) can be defined as $2\theta_n$, which represents the geometric phase retardation of the proposed optical system. This geometric phase retardation was equivalent to two times the transmission axis angle of the linear polarizers in the polarization sensor. Because the transmission angles of the linear polarizers in the polarization sensor are fixed at $\theta_n = [0, \pi/4, \pi/2, 3\pi/4]$, this enables the extraction of four self-interference holograms with phase-shifting values of $\delta_n = 2\theta_n = [0, \pi/2, \pi, 3\pi/2]$ in 90° increments from a single-shot image captured by the polarization sensor. A four-phase shifting algorithm was applied to the proposed method to obtain a complex-valued hologram (U_h) from the four extracted self-interference holograms (I_1 - I_4). Four-phase shifting required phase-shifting value differences of 90° and matched the phase-shifting values (δ_n) in the holograms acquired by the proposed IDH system. The four phase-shifting algorithms are as follows:

$$U_h = (I_3 - I_1) - j(I_4 - I_2). \quad (11)$$

Consequently, bias and conjugate noise-removed complex-valued hologram information can be acquired in the proposed IDH system using a single-shot phase-shifting algorithm.

TABLE 1 Jones matrices for optical components.

	Jones transfer matrix	Optical components
$T_{Q(45)}$	$\frac{1}{\sqrt{2}} \begin{bmatrix} 1 & j \\ j & 1 \end{bmatrix}$	Quarter-wave plate, azimuth angle at 45°
$T_{Q(-45)}$	$\frac{1}{\sqrt{2}} \begin{bmatrix} 1 & -j \\ -j & 1 \end{bmatrix}$	Quarter-wave plate, azimuth angle at -45°
$T_{PBS(p)}$	$\begin{bmatrix} 1 & 0 \\ 0 & 0 \end{bmatrix}$	Polarization beam splitter, transmitted
$T_{PBS(s)}$	$\begin{bmatrix} 0 & 0 \\ 0 & 1 \end{bmatrix}$	Polarization beam splitter, reflected
T_M	$\begin{bmatrix} 1 & 0 \\ 0 & -1 \end{bmatrix}$	Mirror
$T_{L(\theta)}$	$\begin{bmatrix} \cos^2\theta_n & \cos\theta_n \sin\theta_n \\ \cos\theta_n \sin\theta_n & \sin^2\theta_n \end{bmatrix}$	Linear polarizer

3 | RESULTS

3.1 | Experimental setup

We constructed an experimental setup to verify the proposed single-shot phase-shifting IDH optical system (Figure 2). A bandpass filter (Thorlabs, FBH520-10), which has a central wavelength of 520 nm and spectral bandwidth of 10 nm, a QWP (Thorlabs, WPQ10ME-532) for a wavelength of 532 nm, and a monochromatic polarization sensor (Lucid Vision, PHX050S1), which has 2448×2048 pixels with a $3.45 \mu\text{m}$ pitch, were used in the experimental setup. Additional 4-f relay optics were located between the interferometer optics and polarization sensor in the implemented experimental setup, which differs from the schematic illustration shown in Figure 1. The 4-f relay optic is necessary to reduce the magnification of the proposed optical system and obtain a sufficient field of view for the object scene. The distance z_h should be decreased to reduce optical magnification, as defined in Equation (2). The optical field on the mirror surface was imaged using 4-f optic to z_h , away from the polarization sensor plane. The z_h value cannot be smaller than the size of the polarization beam splitter if the 4-f optic are not introduced in the experimental setup. The focal lengths of the field lens (f_o), concave mirror (f_c), lenses in the 4-f optic, and distances z_l and z_h were set as 150, 200, 100, 100, and 10 mm, respectively. All optical components in the experimental setup had a clear aperture size of 25 mm. The dimensions of the interferometer, including the optical mounts (enlarged in the inset of Figure 2), were $175 \text{ mm} \times 100 \text{ mm}$. Two 10 mm dice were

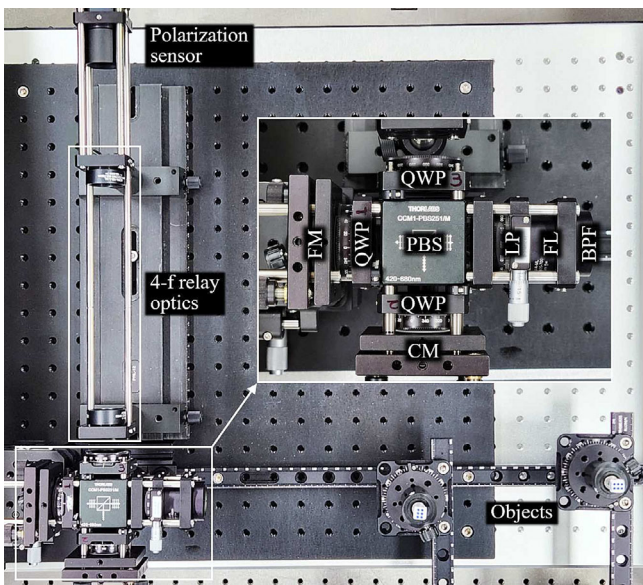


FIGURE 2 Photograph of experimental setup for demonstration.

used as objects in the scene. The object distance (z_o) for the front dice and the distance between the two dice were set to 200 mm and 150 mm, respectively. White light-emitting diodes with a power of 3 W and color temperature of 6000K were used as incoherent light sources for each dice object. The magnification factors defined in (6) for this experimental setup were calculated to be 0.06.

The complex-valued hologram (U_h) obtained from (11) was numerically reconstructed to retrieve the field on the object scene plane (U_z) using the angular spectrum propagation method [26]. The backpropagation of U_h on the hologram plane to U_z on the object scene plane (where z_r departs from the hologram plane) can be performed based on the following equation,

$$U_r(x, y) = F^{-1} \left[F[U_h(x, y)] \exp \left\{ jk_0 z_r \sqrt{1 - \lambda^2 (k_x^2 + k_y^2)} \right\} \right], \quad (12)$$

where $k_o = 2\pi/\lambda$ and (k_x, k_y) are the wavenumber- and frequency-domain coordinates of the U_h -field, respectively. The images of the numerically reconstructed results presented in this section indicated the intensity of the object scene plane ($|U_r|^2$). The hologram information captured in the experimental setup may exhibit phase aberrations owing to imperfections in the optical system and alignment errors. Phase aberrations were compensated by applying a sparse optimization technique [27, 28] during the numerical reconstruction procedure.

3.2 | Experimental results

The single-shot four-phase shifting results of the proposed method for the experimental setup are shown in Figures 3 and 4. Figure 3 shows the results of the single-shot acquired four phase-shifted holograms, and Figure 4 presents numerically reconstructed images of the object scene from the complex-valued hologram extracted by the four phase-shifting algorithm.

A polarization sensor consists of a set of polarizer arrays in the form of a 2×2 pixel array with four linear polarization angles and a 45° difference. Therefore, four phase-shifted hologram images could be extracted from a raw image file acquired by the polarization sensor using a suitable sampling method. The phase-shifted holograms extracted from the image captured by the polarization sensor in the proposed optical system are shown in Figure 3A. The four extracted phase-shifted hologram images have a phase retardation difference of 90° , which is equal to two times the transmission axis angle of the linear polarizers in the polarization sensor as expressed by (10). A complex-valued hologram can be obtained by

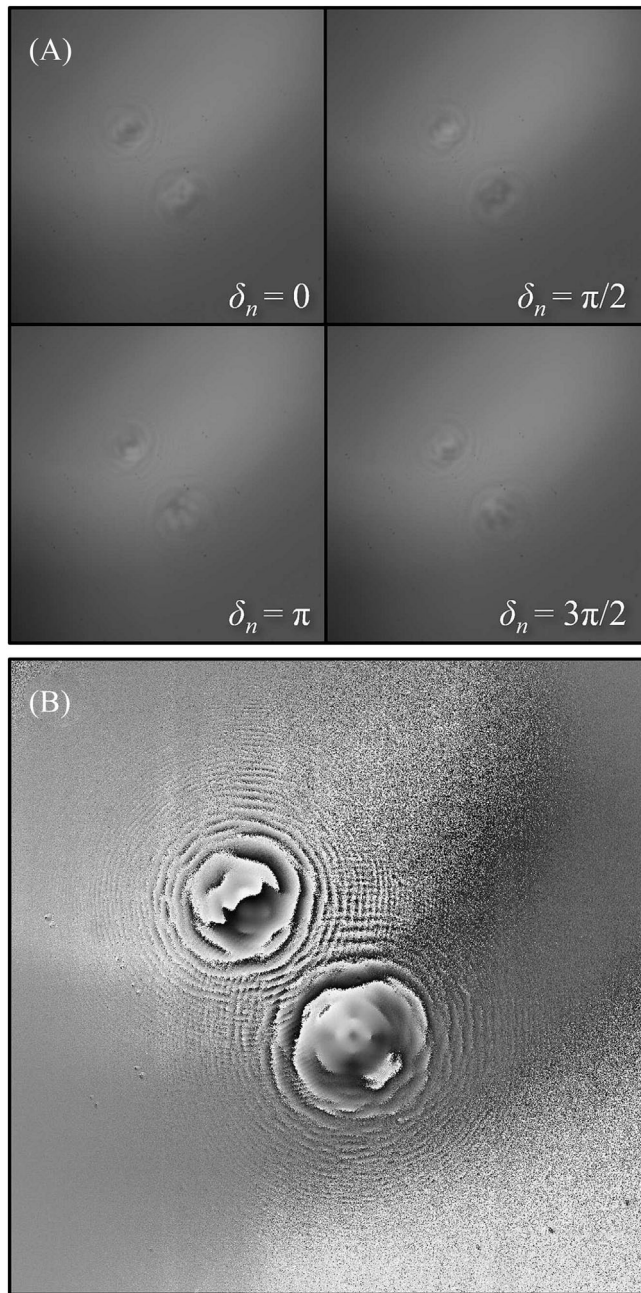


FIGURE 3 (A) Four single-shot hologram images with different phase retardation captured by the polarization sensor and (B) phase-angle representation of complex-valued hologram extracted by the four phase-shifting algorithm.

applying the four-phase shifting technique to these images expressed by (11). The phase angle distribution used to visualize the extracted complex-valued hologram is shown in Figure 3B.

The results of the numerical reconstruction focusing on each die in the scene are shown in Figure 4A,B. In these figures, the dice at the front and back, marked by the red and blue squares, respectively, are enlarged in the inset to compare the reconstruction depths. “Video 1” is a

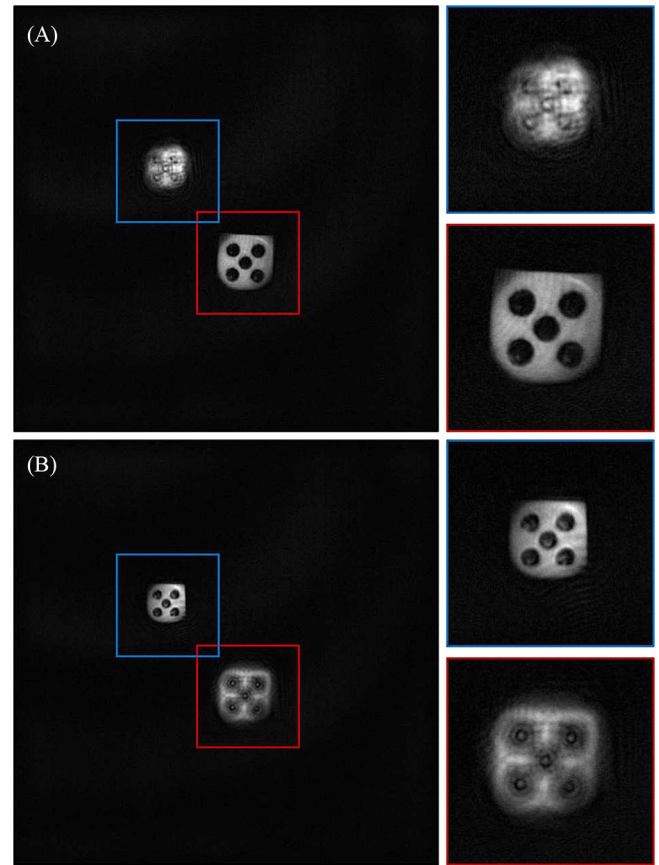


FIGURE 4 Numerically reconstructed image from the complex-valued hologram focused on (A) front and (B) back dice (see “Video 1”).

movie of the numerical reconstructions shown in Figure 4. In this video, the reconstruction depth changes in the object scene are visualized while varying the reconstruction depth from 150 mm to 200 mm at 1 mm intervals. The reconstruction depths for the front and back dices observed in the experiment were 183 mm and 167 mm, respectively, which are consistent with the reconstruction depths (z_r) calculated using (5).

As the phase-shifting technique can be applied to single-shot images acquired using the proposed method, hologram movies of dynamic scenes can be recorded using the same optical system. A hologram of the dynamic scene of the rotating front dice was recorded at 24 frames per second, which was the maximum frame rate of the polarization sensor. The resultant phase angle and numerical reconstruction images focusing on the front and back dice from frames 1 to 19 with three-frame intervals in the recorded hologram movie are shown in Figure 5A–C. The phase angles and numerically reconstructed videos are shown in “Video 2.”

These results verify that the proposed single-shot phase-shifting method in Michelson-based IDH can acquire holographic information free of bias and

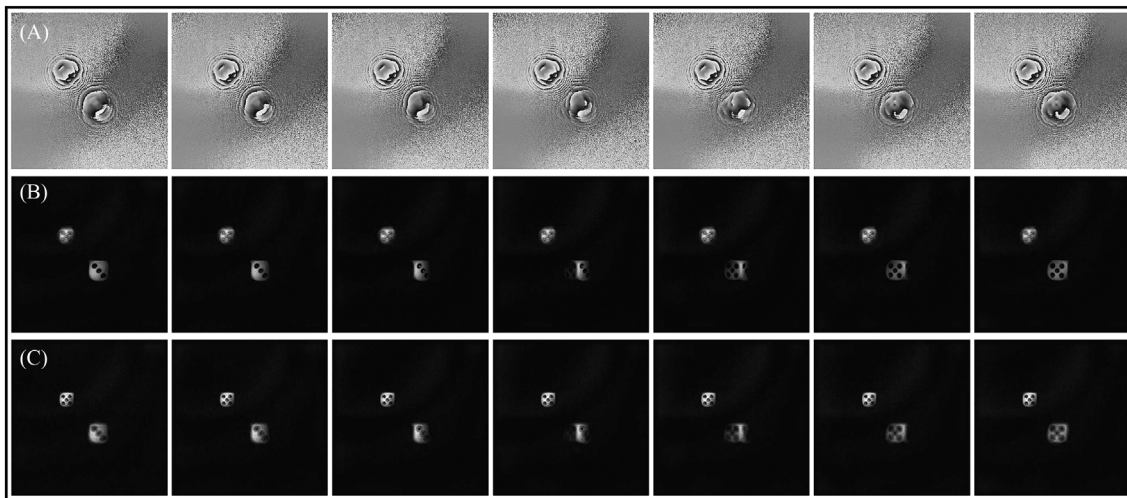


FIGURE 5 Single-frame excerpts (frames 1 to 19 at three-frame intervals) from recorded hologram movie: (A) phase-angle representation of the complex hologram, numerical reconstruction focused on the (B) front and (C) back objects (see “Video 2”).

conjugate image noise within a single acquisition. Notably, our method demonstrates its capacity to record holographic movies seamlessly. Although bias and conjugate noise were effectively removed, the numerical reconstruction results showed the presence of noise in the object and background. This noise is thought to be mainly caused by the fact that the quadratic phase used as the transfer function in the numerical reconstruction does not exactly match the transfer function of the actual interferometer. Other possible sources of noise include polarization aberrations caused by less-than-ideal polarization-modulating optical elements, optical misalignment in the experimental setup, and vibration issues during IDH acquisition.

4 | CONCLUSION

In conclusion, our research presented a novel approach for optical systems based on Michelson interferometry using a single-shot phase-shifting method. This method was specifically designed to facilitate the real-time acquisition of self-interference incoherent holograms. To achieve the desired geometric phase retardation, our optical system incorporated additional polarization-modulating elements, such as a linear polarizer, QWP, and polarization beam splitter. This distinguishes it from conventional Michelson-based IDH optical systems. In addition to these optical components, we integrated a polarization sensor into our setup, which allowed for the simultaneous acquisition of four holograms with distinct geometric phase differences in a single-exposure acquisition. This feature enabled the proposed method to eliminate effectively bias and conjugated noise terms from the acquired incoherent hologram data in

real-time. This was achieved by applying four phase-shifting techniques to single-shot-captured geometric phase-shifted holograms. An experimental setup was constructed to validate the proposed method. Using this setup, we demonstrate the real-time recording of incoherent hologram movies using the proposed method. The results of these experiments, which included single-shot phase shifting and real-time acquisition of hologram sequences, clearly confirm the feasibility of the proposed method. Experimental results were obtained under monochromatic conditions at a wavelength of 532 nm. Because the wavefront modulation elements used in the proposed method are mirrors and are not wavelength-dependent, it is expected that they can be extended to full-color IDH by replacing the wave plates and lenses with achromatic elements.

The proposed method does not require an off-axis configuration to eliminate bias/conjugate noise and can be implemented using simple inline optical structures. Because it uses geometric phase shifting, it has the advantage of avoiding mechanical motion devices, such as piezo transducers or rotators. An additional advantage is that simple mirrors can be used for wavefront modulation optics rather than phase gratings, birefringence, geometric phases, or liquid-crystal-based optics. The proposed method enables real-time Michelson interferometry-based IDH imaging while maintaining the advantages of an easy optical configuration with simple optical components. Furthermore, the image quality of the captured hologram can be improved by reducing vibrations during the sequential recording process in previous studies. Therefore, the proposed method is expected to be utilized in various IDH applications that require Michelson interferometry configurations in real-time.

ACKNOWLEDGMENTS

This work was supported by the Institute of Information & Communications Technology Planning & Evaluation (IITP) grant funded by the Korea Government (MSIT) (no. 2019-0-00001, Development of Holo-TV Core Technologies for Hologram Media Services).

CONFLICT OF INTEREST STATEMENT

The author declares that there are no conflicts of interest.

ORCID

Keehoon Hong  <https://orcid.org/0000-0001-7325-1036>

REFERENCES

- J. Rosen, A. Vijayakumar, M. Kumar, M. R. Rai, R. Kelner, Y. Kashter, A. Bulbul, and S. Mukherjee, *Recent advances in self-interference incoherent digital holography*, *Adv. Opt. Photonics* **11** (2019), no. 1, 1–66, DOI [10.1364/AOP.11.000001](https://doi.org/10.1364/AOP.11.000001).
- T. Tahara, Y. Zhang, J. Rosen, V. Anand, L. Cao, J. Wu, T. Koujin, A. Matsuda, A. Ishii, Y. Kozawa, R. Okamoto, R. Oi, T. Nobukawa, K. Choi, M. Imbe, and T.-C. Poon, *Roadmap of incoherent digital holography*, *Appl. Phys. B* **128** (2022), no. 11, DOI [10.1007/s00340-022-07911-x](https://doi.org/10.1007/s00340-022-07911-x).
- J. Rosen, N. Siegel, and G. Brooker, *Theoretical and experimental demonstration of resolution beyond the Rayleigh limit by FINCH fluorescence microscopic imaging*, *Opt. Express* **19** (2011), no. 27, 26249–26268, DOI [10.1364/OE.19.026249](https://doi.org/10.1364/OE.19.026249).
- M. K. Kim, *Full color natural light holographic camera*, *Opt. Express* **21** (2013), no. 8, 9636–9642, DOI [10.1364/OE.21.009636](https://doi.org/10.1364/OE.21.009636).
- V. Bianco, M. Paturzo, A. Finizio, and P. Ferraro, *Off-axis self-reference digital holography in the visible and far-infrared region*, *ETRI J.* **41** (2019), no. 1, 84–92, DOI [10.4218/etrij.2018-0420](https://doi.org/10.4218/etrij.2018-0420).
- J. Hong and M. K. Kim, *Single-shot self-interference incoherent digital holography using off-axis configuration*, *Opt. Lett.* **38** (2013), no. 23, 5196–5199, DOI [10.1364/OL.38.005196](https://doi.org/10.1364/OL.38.005196).
- O. Mudanyali, D. Tseng, C. Oh, S. O. Isikman, I. Sencan, W. Bishara, C. Oztoprak, S. Seo, B. Khademhosseini, and A. Ozcan, *Compact, light-weight and cost-effective microscope based on lensless incoherent holography for telemedicine applications*, *Lab. Chip* **10** (2010), no. 11, 1417–1428. <https://pubs.rsc.org/en/content/articlelanding/2010/lc/c000453g>
- W. Chen, C. Quan, and C. J. Tay, *Extended depth of focus in a particle field measurement using a single-shot digital hologram*, *Appl. Phys. Lett.* **95** (2009), no. 20, 201103, DOI [10.1063/1.3263141](https://doi.org/10.1063/1.3263141).
- J. Rosen and G. Brooker, *Digital spatially incoherent Fresnel holography*, *Opt. Lett.* **32** (2007), no. 8, 912–914, DOI [10.1364/OL.32.000912](https://doi.org/10.1364/OL.32.000912).
- K. Choi, J. Yim, S. Yoo, and S.-W. Min, *Self-interference digital holography with a geometric-phase hologram lens*, *Opt. Lett.* **42** (2017), no. 19, 3940–3943, DOI [10.1364/OL.42.003940](https://doi.org/10.1364/OL.42.003940).
- K. Choi, K.-I. Joo, T.-H. Lee, H.-R. Kim, J. Yim, H. Do, and S.-W. Min, *Compact self-interference incoherent digital holographic camera system with real-time operation*, *Opt. Express* **27** (2019), no. 4, 4818–4833, DOI [10.1364/OE.27.004818](https://doi.org/10.1364/OE.27.004818).
- R. Kumar, V. Anand, and J. Rosen, *3D single shot lensless incoherent optical imaging using coded phase aperture system with point response of scattered airy beams*, *Sci. Rep.* **13** (2023), no. 1, 2996, DOI [10.1038/s41598-023-30183-0](https://doi.org/10.1038/s41598-023-30183-0).
- T. Nobukawa, Y. Katano, M. Goto, T. Muroi, K. Hagiwara, and N. Ishii, *Grating-based in-line geometric-phase-shifting incoherent digital holographic system toward 3D videography*, *Opt. Express* **30** (2020), no. 15, 27825–27840, DOI [10.1364/OE.460187](https://doi.org/10.1364/OE.460187).
- S. Sakamaki, N. Yoneda, and T. Nomura, *Single-shot in-line Fresnel incoherent holography using a dual-focus checkerboard lens*, *Appl. Opt.* **59** (2020), no. 22, 6612–6618, DOI [10.1364/AO.393176](https://doi.org/10.1364/AO.393176).
- N. Siegel and G. Brooker, *Single shot holographic super-resolution microscopy*, *Opt. Express* **29** (2021), no. 11, 15953–15968, DOI [10.1364/OE.424175](https://doi.org/10.1364/OE.424175).
- A. Vijayakumar, T. Katkus, S. Lundgaard, D. P. Linklater, E. P. Ivanova, S. H. Ng, and S. Juodkazis, *Fresnel incoherent correlation holography with single camera shot*, *Opto-Electron. Adv.* **3** (2020), no. 8, 200004, DOI [10.29026/oea.2020.200004](https://doi.org/10.29026/oea.2020.200004).
- T. Tahara, T. Kanno, Y. Arai, and T. Ozawa, *Single-shot phase-shifting incoherent digital holography*, *J. Opt.* **19** (2017), no. 6, 65705, DOI [10.1088/2040-8986/aa6e82](https://doi.org/10.1088/2040-8986/aa6e82).
- K. Choi, K. Hong, J. Park, and S.-W. Min, *Michelson-interferometric-configuration-based incoherent digital holography with a geometric phase shifter*, *Appl. Opt.* **59** (2020), no. 7, 1948–1953, DOI [10.1364/AO.383118](https://doi.org/10.1364/AO.383118).
- G. Pedrini, H. Li, A. Faridian, and W. Osten, *Digital holography of self-luminous objects by using a Mach Zehnder setup*, *Opt. Lett.* **37** (2012), no. 4, 713–715, DOI [10.1364/OL.37.000713](https://doi.org/10.1364/OL.37.000713).
- K. Choi, J.-W. Lee, J. Shin, K. Hong, J. Park, and H.-R. Kim, *Real-time noise-free inline self-interference incoherent digital holography with temporal geometric phase multiplexing*, *Photonics Res.* **11** (2023), no. 6, 906–916, DOI [10.1364/PRJ.476354](https://doi.org/10.1364/PRJ.476354).
- T. Tahara, *Polarization-filterless polarization-sensitive polarization-multiplexed phase-shifting incoherent digital holography (P⁴IDH)*, *Opt. Lett.* **48** (2023), no. 15, 3881–3884, DOI [10.1364/OL.491990](https://doi.org/10.1364/OL.491990).
- T. Muroi, T. Nobukawa, Y. Katano, and K. Hagiwara, *Capturing videos at 60 frames per second using incoherent digital holography*, *Opt. Continuum* **2** (2023), no. 11, 2409–2420, DOI [10.1364/OPTCON.504455](https://doi.org/10.1364/OPTCON.504455).
- M. Novak, J. Millerd, N. Brock, M. North-Morris, J. Hayes, and J. Wyant, *Analysis of a micropolarizer array-based simultaneous phase-shifting interferometer*, *Appl. Opt.* **44** (2005), no. 32, 6861–6868, DOI [10.1364/AO.44.006861](https://doi.org/10.1364/AO.44.006861).
- C. Zhang, H. Zhu, and B. Zhao, *The tempo-spatially modulated polarization atmosphere Michelson interferometer*, *Opt. Express* **19** (2011), no. 10, 9626–9635, DOI [10.1364/OE.19.009626](https://doi.org/10.1364/OE.19.009626).
- T. Nobukawa, Y. Katano, M. Goto, T. Muroi, N. Kinoshita, Y. Iguchi, and N. Ishii, *Incoherent digital holography simulation based on scalar diffraction theory*, *JOSA A* **38** (2021), no. 7, 924–932, DOI [10.1364/JOSAA.426579](https://doi.org/10.1364/JOSAA.426579).
- H.-J. Yeom, S. Cheon, K. Choi, and J. Park, *Efficient mesh-based realistic computer-generated hologram synthesis with polygon resolution adjustment*, *ETRI J.* **44** (2022), no. 1, 85–93, DOI [10.4218/etrij.2021-0208](https://doi.org/10.4218/etrij.2021-0208).

27. Y. Kim, K. Hong, H.-J. Yeom, K. Choi, J. Park, and S.-W. Min, *Wide-viewing holographic stereogram based on self-interference incoherent digital holography*, *Opt. Express* **30** (2022), no. 8, 12760–12774, DOI [10.1364/OE.454835](https://doi.org/10.1364/OE.454835).
28. Z. Ren, J. Zhao, and E. Y. Lam, *Automatic compensation of phase aberrations in digital holographic microscopy based on sparse optimization*, *APL Photonics* **4** (2019), no. 11, 110808, DOI [10.1063/1.5115079](https://doi.org/10.1063/1.5115079).

AUTHOR BIOGRAPHIES



Keehoon Hong received his Ph.D. degree in Electrical Engineering and Computer Science from Seoul National University, Seoul, Republic of Korea in 2014. Since 2015, he has worked at the Electronics and Telecommunications Research Institute (ETRI), Daejeon, Republic of Korea, where he is currently the Director of the Digital Holography Research Section. His research interests include autostereoscopic three-dimensional displays, digital holographic displays, and holographic optical elements.



Kihong Choi received his Ph.D. degree in Information Display from Kyunghee University, Seoul, Republic of Korea in 2019. He is currently a Senior Researcher at the Digital Holography Research Section of the Electronics and Telecommunications Research Institute (ETRI), Daejeon, Republic of Korea. His research interests include digital holographic acquisition and display systems.

SUPPORTING INFORMATION

Additional supporting information can be found online in the Supporting Information section at the end of this article.

How to cite this article: K. Hong and K. Choi, *Single-shot phase-shifting on Michelson interferometry for incoherent digital holography*, *ETRI Journal* (2024), 1–10, DOI [10.4218/etrij.2023-0396](https://doi.org/10.4218/etrij.2023-0396).